SCANNING VOL. 37, 23–35 (2015)

Investigation of Temperature Induced Mechanical Changes in Supported Bilayers by Variants of Tapping Mode Atomic Force Microscopy

Nicole Shamitko-Klingensmith[1,2] and Justin Legleiter[1,2,3]

[1]The C. Eugene Bennett Department of Chemistry, West Virginia University, Morgantown, West Virginia
[2]NanoSAFE, West Virginia University, Morgantown, West Virginia
[3]The Center for Neurosciences, West Virginia University, Morgantown, West Virginia

Summary: Tapping mode atomic force microscopy (AFM) is an invaluable technique for examining topographical features of biological materials in solution, and there has been a growing interest in developing techniques to provide further compositional contrast and information concerning surface mechanical properties. Phase shifts, cantilever response at higher harmonic frequencies of the drive, and time-resolved tip/sample force reconstruction have all been shown to provide additional compositional contrast of surfaces, as compared to basic tapping mode AFM imaging. This study aimed to demonstrate the relative ability of these different imaging techniques to detect temperature induced changes in the elastic modulus of supported total brain lipid extract (TBLE) bilayer patches on mica. To aid in direct comparison between the different imaging techniques, all required data was obtained simultaneously while capturing traditional tapping mode AFM topography images. While all of the techniques were able to provide compositional contrast consistent with known temperature-induced changes in the bilayer patch, interpretation of the resulting contrast was not always straightforward. Phase imaging suffered from contrast inversion. Individual harmonics responded in a variety of ways to the temperature-induced changes in elastic modulus of the bilayer. The maximum tapping force (or peak force) associated with imaging the bilayer correctly reflected the changes in elastic modulus of the lipid bilayer. Importantly, as the required data can be obtained simultaneously, combining these different imaging techniques can lead to a more complete understanding of a sample's mechanical features. SCANNING 37:23–35, 2015.

Key words: atomic force microscopy, lipid bilayer, higher harmonic imaging, scanning probe acceleration microscopy, force reconstruction, phase transition

Introduction

Atomic force microscopy (AFM) has become a standard technique for imaging surfaces with nanoscale spatial resolution. A widely used dynamic AFM imaging technique for soft materials in solution is the tapping mode, which effectively eliminates larger lateral forces associated with contact mode AFM (Hansma *et al.*, 1994; Putman *et al.*, 1994). In tapping mode, images are obtained by systematically monitoring the oscillation amplitude of a cantilever affixed with an ultrasharp tip probe that physically interacts with the sample by intermittently making contact with the surface. The cantilever is commonly driven near its resonance frequency ω_0 by a variety of means (Revenko and Proksch, 2000; Herruzo and Garcia, 2007). As the surface acts as a repulsive barrier, the intermittent contact between the tip and sample results in a decrease in the cantilever oscillation from a "free" amplitude A_0 to a tapping amplitude A. The surface topography is determined by raster scanning the tip across the surface and implementation of a feedback loop that continuously corrects the vertical extension of the piezoelectric scanner to maintain a constant set point ratio, $s = A/A_0$. As a result of maintaining this set point, the AFM images surfaces in the tapping mode by trying to maintain the total force between the tip and surface in one oscillation

Contract grant sponsor: Brodie Entrepreneurial and Development Fund. Contract grant sponsor: National Science Foundation; Contract grant number: CMMI1054211; Contract grant sponsor: Integrative Graduate Education and Research Traineeship; Contract grant number: DGE-1144676; Contract grant sponsor: WVU NanoSAFE; Contract grant number: 1003907.

Address for reprints: Justin Legleiter, 217 Clark Hall, The C. Eugene Bennett Department of Chemistry, West Virginia University, Morgantown, WV 26505.
E-mail: justin.legleiter@mail.wvu.edu

Received 28 July 2014; revised 28 September 2014; Accepted with revision 6 October 2014

DOI: 10.1002/sca.21175
Published online 4 November 2014 in Wiley Online Library (wileyonlinelibrary.com).

cycle at a constant value (Kowalewski and Legleiter, 2006; Melcher *et al.*, 2008).

Considerable effort has been made to develop techniques based on tapping mode AFM to simultaneously determine mechanical properties of surfaces while obtaining traditional topographic images. These approaches offer several potential advantages over other traditional AFM techniques that measure mechanical properties, such as high spatial resolution and relatively nondestructive imaging forces associated with tapping mode. Due to the large deformation of soft samples required by other methods to measure mechanical properties of surfaces (i.e., force volume imaging and nano-indentation), these techniques can suffer from decreased spatial resolution and potentially damage the surface. This is particularly relevant to the application of AFM to study fragile biological samples in solution.

In this regard, numerous variations of tapping mode AFM have been developed to simultaneously capture morphological and mechanical information of surfaces. One of the first such variations was phase-contrast imaging, which is based on measuring the phase difference between the drive signal and the cantilever motion (Cleveland *et al.*, 1998; Anczykowski *et al.*, 1999). Further insight into the mechanical properties of a sample are obtainable by analysis of the cantilever deflection trajectory at higher harmonic frequencies with respect to the drive frequency (Hillenbrand *et al.*, 2000; Stark and Hecki, 2003). When applying a harmonic drive to the cantilever, the resulting harmonic oscillation of the cantilever is distorted by the tapping event during each oscillation cycle (Hillenbrand *et al.*, 2000; Stark and Hecki, 2003; Legleiter *et al.*, 2006; Preiner *et al.*, 2007). This results in some power being shifted to these higher harmonic frequencies. Mapping of the cantilever response at higher harmonics has been shown to provide additional compositional contrast when imaging in liquids (Preiner *et al.*, 2007; Xu *et al.*, 2009). More recently, reconstructing the time-resolved tip/sample imaging force while capturing tapping mode AFM images has garnered considerable attention as a method to gain mechanical information about the sample. Stark et al. first converted the cantilever deflection signal into time-resolved tip/sample forces by taking the inverse Fourier transform of the Fourier-transformed cantilever trajectory divided by its transfer function (Stark *et al.*, 2002), and since then several other methods have been proposed and developed to obtain time-resolved tip/sample forces associated with tapping mode AFM (Sahin *et al.*, 2004; Legleiter e*t al.*, 2006; Dong *et al.*, 2009; Sarioglu and Solgaard, 2011; Garcia and Herruzo, 2012; Sarioglu *et al.*, 2012). One of these methods, scanning probe acceleration microscopy (SPAM), treats the cantilever as an accelerometer from which the tip/sample forces can be extracted during regular operation without the need for specially designed cantilevers (Legleiter *et al.*, 2006). SPAM utilizes the second derivative of the deflection signal to recover the tip acceleration trajectory, and this is converted into the time-resolved tip/sample force.

Due to the ability to perform tapping mode AFM experiments in aqueous environments, it has been widely applied to the study of biologically relevant samples and surfaces. Extensive AFM experiments have been performed on supported lipid bilayers, which act as models of cellular membranes (Leonenko *et al.*, 2006; Milhiet *et al.*, 2006; Legleiter *et al.*, 2011; Pifer *et al.*, 2011; Shamitko-Klingensmith *et al.*, 2012). Membranes are essential components of all living systems, and a variety of biochemical reactions occur at these surfaces. Cellular membranes have a two-dimensional liquid-crystalline structure and are typically comprised of a diverse mixture of amphiphilic lipid components (vanMeer *et al.*, 2008; Espinosa *et al.*, 2011). Mechanical properties of cellular membranes are vital to the maintenance of normal cellular function, as membranes must maintain high lateral fluidity while also retaining structural integrity. The mechanical properties of lipid membranes, such as fluidity, depend on lipid composition and local environmental properties such as pressure, hydration, pH, and temperature (Kranenburg and Smit, 2005; Suresh and Edwardson, 2010). Under physiological conditions, lipid membranes are predominantly in a fluid phase; however, thermal fluctuations can alter the phase state of membranes. In general, increasing temperature causes lipid membranes to enter a more disordered state, whereas lowering the temperature encourages a more ordered, potentially nonfluid state (Mansilla *et al.*, 2004). Phase transitions occur at a variety of temperatures for different lipid systems based on the packing efficiency of specific lipid components (vanMeer *et al.*, 2008). Changes in lipid organization profoundly influence cellular functions, such as signal transduction and membrane trafficking (Simons and Vaz, 2004; vanMeer *et al.*, 2008).

Here, the ability of phase imaging, imaging based on the cantilever response at specific higher harmonic frequencies, and reconstruction of the time-resolved tapping forces are evaluated on their ability to track temperature-induced mechanical changes and phase transitions of supported lipid bilayers. Time-resolved tapping forces were recovered using SPAM. All of these imaging modes can be obtained simultaneously, which allows for direct comparison within individual tapping mode AFM experiments. For these experiments, patches of total brain lipid extract (TBLE) bilayers containing 30% exogenous cholesterol and supported on a mica substrate were imaged in solution. Patches of bilayers were used so that the exposed mica substrate could act as an internal standard for the different imaging techniques.

Experimental Procedures

Sample Preparation

TBLE (Avanti Polar Lipids) and cholesterol were dissolved in chloroform (ACROS Organics) to a concentration of 70% TBLE and 30% cholesterol by mass. The chloroform was removed using a Vacufuge (Eppendorf), and the resulting lipid films were resuspended in phosphate buffered saline (PBS) (pH 7.3) at a concentration of 1 mg/mL. Five sequential freeze–thaw cycles in liquid nitrogen were performed to promote bilayer formation. The lipid suspensions were then placed in a bath sonicator for 20 min to promote vesicle formation. The ensuing vesicle solution was diluted 50 times. 5 μL of this diluted solution was injected directly into the AFM fluid cell, which already contained 35 μL of PBS, and onto a freshly cleaved mica substrate. Supported lipid bilayer patches formed on the mica surface within a few minutes.

AFM Imaging Conditions

In situ AFM experiments were performed with a Nanoscope V Multimode scanning probe microscope (Veeco, Santa Barbara, CA) using a fluid cell equipped with an O-ring and a V-shaped oxide-sharpened silicon nitride cantilever (Budget Sensors). All topography images were acquired in the tapping mode with acoustic excitation of the cantilever. While the nominal spring constant of the cantilevers provided by the manufacturer was 0.27 N/m, the actual spring constant of the cantilevers used in this study were calculated using a thermal tuning method, as previously described (Hutter and Bechhoefer, 1993). All images were acquired using a closed-loop "vertical engage" J-scanner. The scan rate was 1.95 Hz with cantilever drive frequencies ranging from approximately 8 to 9 kHz. The free amplitude of the cantilever was 29.4 nm for all experiments presented here, and the set point ratio, defined as the tapping amplitude to the free amplitude, was maintained at 0.8. Images were captured at 5×1.25 μm and 512×128 pixel resolutions. Topography and phase images were captured using the software supplied by the manufacturer. The temperature was varied from 28 to 37 °C using the Bio-Heater accessory for the multimode AFM (Veeco, Santa Barbara, CA) and additionally monitored with a thermister incorporated into the fluid cell.

Higher Harmonic Imaging and Scanning Probe Acceleration Microscopy Imaging

Entire cantilever deflection trajectories were simultaneously captured during acquisition of each tapping mode AFM image by use of a signal access module (Veeco), a CompuScope 14-Bit A/D Octopus data acquisition card (Gage Applied Technologies, Lachine, QB, Canada), and custom-written software. Trajectories were captured at 2.5 MS/s and 14-bit resolution with a vertical resolution of ±2 V. These cantilever trajectories were processed using Matlab equipped with the signal processing toolbox (Mathworks, Natick, MA). A sliding window Fourier transform was applied to the cantilever deflection trajectory. The window was six oscillation cycles in length and was advanced by one oscillation cycle at a time. By taking the magnitude of the resulting power spectrums, images based on the response of a single harmonic frequency were constructed by reshaping the resulting response at a given frequency into an appropriately sized matrix corresponding to the AFM image. To reconstruct the time-resolved tip/sample force using scanning probe acceleration microscopy, the cantilever deflection trajectories were also filtered with a Fourier transform based harmonic comb filter using the same sliding window as was employed for generation of harmonic images. In this process intensities corresponding to integer harmonic frequencies are used to reconstruct a deflection signal, $y_{\mathrm{rec}}(t)$, by inverse Fourier transform of the power spectrum based on the following equation:

$$y_{rec}(t) = \hat{f}^{-1}\left[y(\omega)\sum_{k=1}^{N}\delta(\omega - k\omega_{oper})\right] \qquad (1)$$

here $\hat{f}^{-1}$ is the inverse Fourier transform, ω_{oper} is the operating frequency, N is the highest harmonic distinguishable above the noise level (typically 20), and δ is Dirac's delta function (Legleiter *et al.*, 2006). The second derivative of $y_{\mathrm{rec}}(t)$ was taken to obtain the cantilever acceleration, which was multiplied by the effective mass, m_{eff}, of the cantilever to obtain the time-resolved tapping force between the tip and sample based on the following equation,

$$\ddot{y} = \frac{1}{m_{eff}}\left[F_{ext} - b\dot{y} - ky - m_{eff}\omega^2 a_0 \sin(\omega t) + ba_0\omega\cos(\omega t)\right], \qquad (2)$$

which was derived by treating the cantilever motion as a damped driven harmonic oscillator,

$$F_{ext} = m_{eff}\ddot{z} + b\dot{z} + k\left[z - D_0 + a_0\sin(\omega t)\right] \qquad (3)$$

with b being the damping coefficient, k is the cantilever spring constant, z is the position of the cantilever with respect to the surface, D_0 is the resting position of the cantilever base, a_0 is the drive amplitude, and ω is the cantilever's drive frequency. The m_{eff} was estimated based on the calibrated spring constant and resonance

frequency of the cantilever. The position of the cantilever, z, is converted to the cantilever deflection, y, as described by

$$y = z - D_0 + a_0 \sin(\omega t). \quad (4)$$

The maximum tapping force (F_{max}), defined as the peak or largest positive force experienced between the tip and surface during one tapping event, was organized into an appropriately sized matrix corresponding to the AFM image to obtain a spatially resolved force map.

Results and Discussion

Influence of Temperature on Bilayer Height and Phase

To determine the relative applicability of phase imaging, imaging based on the cantilever response at specific higher harmonic frequencies, and reconstruction of the time-resolved tapping forces to study temperature induced mechanical changes in lipid bilayers, tapping mode AFM was performed on supported TBLE bilayer patches. As lipid bilayers have a considerably smaller elastic modulus compared to mica, the bilayer patch on mica is useful for comparing different imaging modes as this system provides a surface with a relatively soft region (supported bilayer) and a hard region (mica) with well-defined morphology (an uncompressed TBLE bilayer is ~4.5–5 nm thick). The supported bilayer patches were imaged at various temperatures (28, 31, 34, and 37 °C) by sequential heating of the sample, and all of the required data for the different imaging variations were obtained simultaneously at each temperature. While this experiment was repeated several times, all representative images presented here were obtained on the same bilayer patch using a single cantilever with a constant drive amplitude, free amplitude, and set point ratio to facilitate comparison between images obtained at different temperatures. This required no adjustment of the cantilever placement within the fluid cell for the duration of the experiment, normalizing errors associated with the geometry of the fluid cell and position of the piezo shaker with respect to the cantilever so that direct comparison from image to image could be made within a single experiment. By keeping these parameters constant, the total tip/sample force per oscillation cycle, F_{total}, remained constant based on the equation:

$$F_{total} \approx 0.5 k a_0 \frac{\Delta A}{A_0}, \quad (5)$$

where k is the spring constant, a_0 is the drive amplitude, ΔA is the tapping amplitude, and A_0 is the free amplitude (Kowalewski and Legleiter, 2006). The experiments presented here were performed with a set point ratio of 0.8. This set point ratio was chosen based on previous studies indicating that this setting was optimal for imaging TBLE bilayer patches on mica (Kumar *et al.*, 2010; Shamitko-Klingensmith *et al.*, 2012). Furthermore, the exposed mica acts as an internal control to verify that F_{total} remained constant and to facilitate direct comparison between images taken at different temperatures (Kumar *et al.*, 2010), and all results are reported relative to this control. While the absolute values of bilayer height, phase shifts, amplitude responses of specific harmonics, and tapping forces from experiment to experiment could vary due to the difficulties in controlling all of the previously mentioned imaging parameters, the relative shifts in these values compared to the internal mica control were consistently reproduced, except in phase imaging as will be discussed later. For simplicity, the results presented here are from one representative replicate of the experiment.

TBLE was chosen for this study as it is a naturally occurring mixture of phospholipids including phosphatidylcholine (PC, 9.6%), phosphatidylethanolamine (PE, 16.7%), phosphatidylinositol (PI, 1.6%), phosphatidylserine (PS, 10.6%), phosphatidic acid (PA, 2.8%), and unknown components comprising 58.7% of the mixture. All of these lipids have varying degrees of saturation which can contribute to the packing arrangement within the lipid membrane. Additionally, 30% exogenous cholesterol was added to the lipid mixture to strengthen the bilayer patches for continual imaging, as previous studies on TBLE containing 0–50% exogenous cholesterol indicated that TBLE bilayers containing 30% exogenous cholesterol have the highest degree of vertical rigidity (Shamitko-Klingensmith *et al.*, 2012). Furthermore, the addition of cholesterol lowers the phase transition temperature of lipid bilayers (Van Dijck *et al.*, 1976; Epand and Bottega, 1987), allowing observation of phase transitions at temperatures accessible by the heated fluid cell. The occurrence of a phase transition is accompanied by significant changes in the mechanical properties of bilayers, providing a simple system to investigate the ability of different imaging techniques to detect such changes.

As a first measurement to determine if a phase transition occurred in the TBLE bilayer patch upon heating, standard tapping mode AFM topography images were used to evaluate fluctuations in bilayer height as a function of temperature (Fig. 1). At 28 °C, the lipid patch had a height of 3.6 ± 0.1 nm (Fig. 1), consistent with previous reports (Kumar *et al.*, 2010; Shamitko-Klingensmith *et al.*, 2012). However, this bilayer height was slightly smaller than the theoretical height of the lipid bilayers (~4.5–5 nm) due to the normal force applied by the cantilever tip compressing the supported bilayer (Kumar *et al.*, 2010). This observed compression was consistent with the bilayer

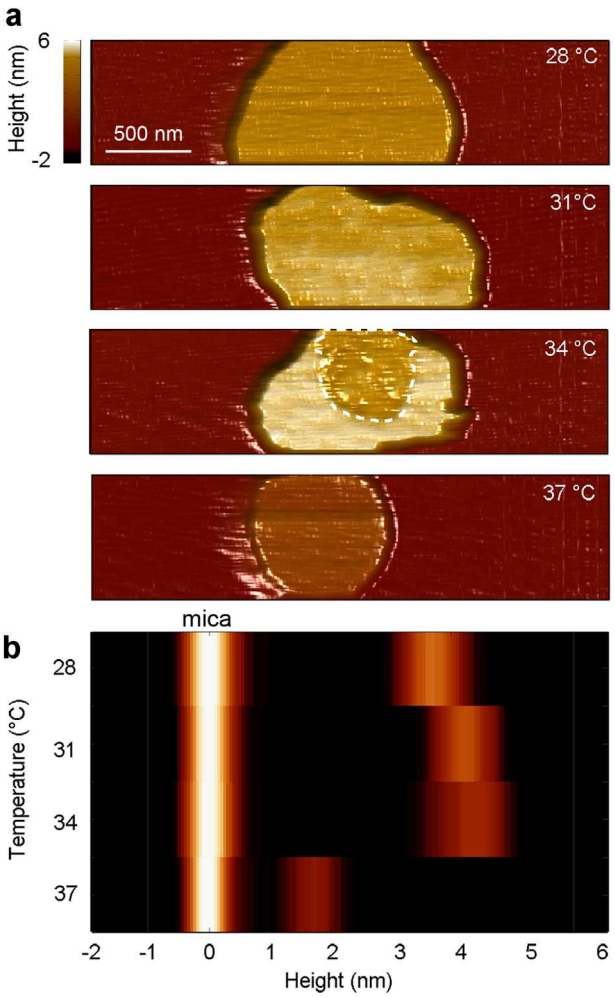

Fig 1. (**a**) AFM topography images of the same TBLE bilayer patch supported on mica taken at 28, 31, 34, and 37 °C. The dotted line in the image taken at 34 °C indicates a region of the bilayer undergoing a phase transition. The color bar is applicable to all images. (**b**) Histograms of all of the height measurements in the AFM images presented as a function of temperature. Brighter colors indicate a larger number of measurements corresponding to a specific height. Measurements corresponding to the mica substrate are indicated.

being a more compliant surface compared to the mica substrate, as has been demonstrated by simulations of complete tapping mode AFM experiments (Shamitko-Klingensmith *et al.*, 2012). As the temperature increased to 31 and 34 °C, the bilayer height slightly increased (4.1 ± 0.5–4.2 ± 0.5 nm, respectively). Further morphological changes within the bilayer patch were apparent at 34 °C as a region of the bilayer had a height that was ~0.7 nm smaller (Fig. 1), indicating the initial stages of a transition to a more compliant phase that is compressed to a greater extent due to the imaging force. As the temperature was further increased to 37 °C, the height of the bilayer patch became considerably smaller (1.8 ± 0.1 nm). At lower temperatures, the lipid components are more tightly packed, resulting in a slightly thicker bilayer, but the change in thickness of bilayers in this temperature range should only be on the order of a few angstroms (Pan *et al.*, 2008; Kučerka *et al.*, 2011). The difference in bilayer height before and after the phase transition is much larger than would be expected due to simple rearrangement of lipid packing. This drastic reduction in height was likely a consequence of the cantilever tip pushing deeper into the more highly fluid bilayer patch, associated with a phase transition occurring in the bilayer. This is consistent with previous reports that demonstrated that changes in observed height of a bilayer measured by tapping mode AFM in solution can be directly related to changes in mechanical and/or adhesive properties of the bilayer (Shamitko-Klingensmith *et al.*, 2012). Unfortunately, there was not a straightforward method to determine the uncompressed height of the bilayer, which is required to obtain a relative value of indentation.

While the same lipid bilayer patch was imaged at the different temperatures, the shape of the patch changed considerably, indicating that the bilayer was quite fluid as expected from the literature (Yip *et al.*, 2001; Shamitko-Klingensmith *et al.*, 2012). As the temperature is raised from 28 °C to 37 °C, the shape (or lateral morphology) of the bilayer patch is also altered (Fig. 1). This could arise from several factors. For example, the time required for the formation of large areas (on the order of 50 by 50 μm or larger) of continuous supported lipid bilayers is significantly reduced under continuous scanning of an AFM tip (Legleiter *et al.*, 2011). This phenomenon is caused by the force exerted by the probe pushing vesicles to the surface, flattening their structure, and promoting vesicle fusion (Jass *et al.*, 2000). While this experiment was performed at low vesicle concentrations to prevent the formation of continuous bilayer, it is still possible that the imaging process actively altered the lateral shape of the bilayer, which can be quite malleable. The lipid patch occupied the largest observable area at 28 °C, but this decreased with increasing temperature. This condensing effect has been noted to occur in order to maintain structural integrity as lateral fluidity of membranes increases and is consistent with studies examining the area of various PC bilayers as a function of temperature (Kučerka *et al.*, 2011).

As the phase of the cantilever operated in tapping mode is commonly used to glean information concerning mechanical properties of surfaces, phase images of the lipid bilayer patches on mica were acquired simultaneously with the topography images at each temperature. The phase images were normalized so that the phase shift associated with tapping events on mica had a value of zero, allowing for direct comparison between phase images taken at different temperatures (Fig. 2). Initially, stark contrast between the mica substrate and the bilayer patch was observed at 28 °C, with the phase shifting 2.1 ± 0.1^0 on the bilayer with respect to the mica substrate. The phase shift associated with the bilayer increased in magnitude with a larger

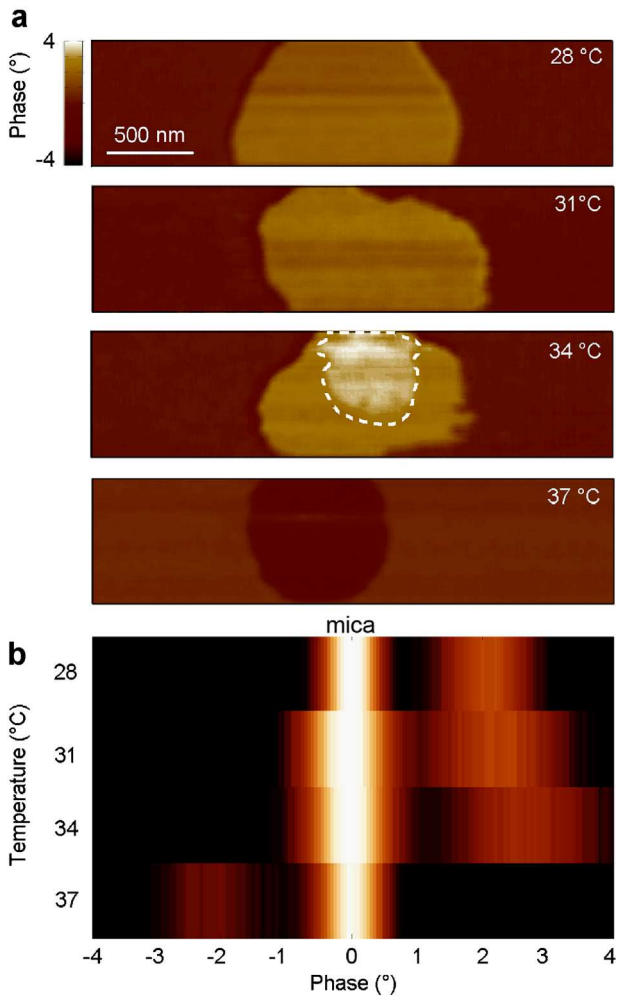

Fig 2. (**a**) AFM phase images of the same TBLE bilayer patch supported on mica taken at 28, 31, 34, and 37 °C. The dotted line in the image taken at 34 °C indicates a region of the bilayer undergoing a phase transition as determined from the topography image shown in Figure 1. The color bar is applicable to all images. (**b**) Histograms of all of the phase measurements in the AFM images presented as a function of temperature. Brighter colors indicate a larger number of measurements corresponding to a specific phase shift. Measurements corresponding to the mica substrate are indicated.

distribution of values as the temperature was raised to 31 and 34 °C (2.5 ± 0.1^0 and 3.1 ± 0.1^0, respectively). Additionally at 34 °C, the region of the bilayer associated with the initial transition to a more fluid state had a clear phase contrast compared with the rest of the bilayer. While at lower temperatures the phase shift associated with the bilayer was always positive, the phase shift associated with the bilayer at 37 °C was negative (-2.3 ± 0.1^0) with respect to the mica substrate. This observed inversion of contrast represents one of the ambiguities related with phase imaging, as the phase contrast between regions of differing elastic modulus are not always consistently in one direction (Bar *et al.*, 1997). The inversion of contrast in the phase images after heating the sample to 37 °C did not occur in every individual replicate of the experiment (Fig. 3). There was, however, always some appreciable change (on the order of 1–3 degrees) in phase contrast when heating a bilayer patch above its transition temperature. Despite the ambiguity in the phase response observed here as a function of temperature, these shifts in phase contrast do indicate that mechanical properties associated with the lipid bilayer patch indeed changed due to the increase in temperature, further supporting the notion that the observed height differences in the topography image are due to a temperature induced phase transition in the lipid bilayer.

Phase contrast is typically associated with tip/sample energy dissipation (Magonov *et al.*, 1997; Cleveland *et al.*, 1998; Garcia *et al.*, 2007). While great strides have been made in the theory underlying phase contrast, especially in solution (Melcher *et al.*, 2009), interpretation of phase images remains difficult due to a variety of competing sources of energy dissipation (i.e., capillary forces (Zitzler *et al.*, 2002), viscoelasticity of the sample (Garcia *et al.*, 1999), and cross talk with topography (Stark *et al.*, 2001)) associated with tip/sample interactions. Phase contrast is also highly dependent on imaging parameters, such as free amplitude and set point ratio (Scott and Bhushan, 2003; Ebeling and Solares, 2013). Changing the set point ratio in tapping

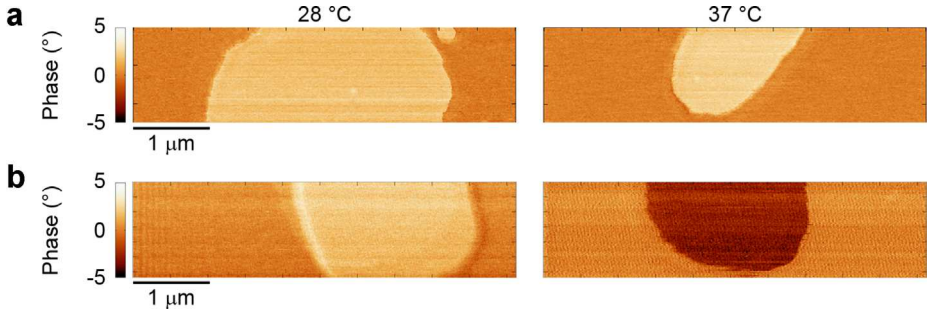

Fig 3. Representative phase images of TBLE bilayer patch supported on mica from two additional experiments demonstrating that the phase shift associated with the transition in the bilayer was inconsistent. That is, in some replicates (**a**) no contrast inversion was observed, while (**b**) contrast inversion was observed in others. Nevertheless, there was always a shift in the phase associated with phase images above 37 °C.

mode AFM can even lead to contrast inversion in phase images for some experimental systems (Bar *et al.*, 1997). As a result, using phase imaging to elucidate mechanical properties of surfaces can be complicated without a priori knowledge of those properties. These issues can be further complicated when operating in solution (Melcher *et al.*, 2009; Ebeling and Solares, 2013). The imaging conditions chosen in this study were optimized for topographical imaging of the bilayer patch, and not phase contrast. It is possible that imaging conditions could be tweaked so that phase images more accurately and reproducibly reflect the relative compressibility of the bilayer patch with respect to mica.

While it would be interesting to correlate changes in phase contrast to the differing ability of the bilayer to dissipate energy before and after undergoing a transition, the relationship between phase contrast and tip/sample dissipation is based on the assumption of cantilever dynamics being dominated by a single eigenmode. However, when operating tapping mode AFM in solution using soft cantilevers ($k < 1$ N/m) with low quality factors ($Q < 5$), the second eigenmode of the cantilever plays a prominent role (Basak and Raman, 2007), and the assumption of a single eigenmode dominating the tip/sample interaction is not met, making it difficult to directly relate phase contrast to tip-sample dissipation alone (Melcher *et al.*, 2009).

As demonstrated by Melcher et al., the phase contrast associated with such soft cantilevers can arise from either (i) energy propagation during the tapping event that excites higher eigenmodes of the cantilever, which is mediated by conservative short-range interactions such as elastic contact forces between the tip and surface, or (ii) tip/sample energy dissipation (Melcher *et al.*, 2009). In our experimental system, which consists of a soft biological lipid bilayer supported on a comparably stiff mica substrate in a high-ionic strength buffer, the DLVO forces are highly screened and adhesion hysteresis is negligible (Voitchovsky *et al.*, 2006; Mueller and Engel, 2007; Melcher *et al.*, 2009). As a result, the observed inversion of contrast in some phase images of the bilayer on mica at 37 °C compared with images taken at different temperatures can be interpreted based on these two sources of phase contrast. At the lower temperatures, the phase contrast is dominated by the momentary propagation of energy from the first to the second eigenmode of the cantilever; whereas, the tip/sample dissipative interaction dominates at 37 °C. Melcher et al. also point out that phase images should not be considered maps of elastic modulus, but rather local stiffness (Melcher *et al.*, 2009).

Observation of Compositional Contrast Using Higher Harmonic Imaging

Due to the nonlinear interaction between the tip and sample during tapping mode AFM, the harmonic motion of the cantilever is distorted during the tapping event, and as a consequence, higher frequencies that are harmonic to the drive frequency are excited within the cantilever (Basak and Raman, 2007). As a result, compositional contrast can be achieved by monitoring harmonic frequencies, and higher harmonic imaging has been used to observe subtle surface features that are difficult to distinguish by ordinary tapping mode AFM experiments (Stark and Hecki, 2003). Application of harmonic imaging is especially useful for imaging in solution, as the large distortion of cantilever motion associated with imaging in liquid leads to a larger excitation of higher harmonics (Preiner *et al.*, 2007).

For this study, AFM images based on the response of specific higher harmonic frequencies were obtained by capturing the entire cantilever deflection trajectory while imaging. Then, using a sliding window Fourier transform, the cantilever response at specific harmonic frequencies was obtained and reshaped into an appropriately sized matrix corresponding to the AFM image. In this way, individual harmonic images can be generated simultaneously for several different harmonic signals of the same TBLE bilayer patch, while raising the temperature from 28 to 37 °C (Figs. 4–8). The first harmonic (data not shown) is analogous to the standard amplitude or error images associated with tapping mode AFM. While the amplitude image is sensitive to the edges of features on the surface and provides important information concerning the efficiency of the feedback loop, it contains little information concerning the mechanical properties of the surface. However, higher harmonics have been used to map a variety of surfaces properties (van Noort *et al.*, 1999; Preiner *et al.*, 2007; Xu *et al.*, 2009). While the results presented here are for one replicate of the experiment, it should be noted that the relative response of the individual harmonics were reproducible from replicate to replicate. That is, the shift of the harmonic response associated with imaging the bilayer patch at each temperature with respect to the internal standard in mica was the same. Due to experimental difficulty in reproducing imaging parameters between replicates, the magnitude of the observed amplitudes associated with harmonics in the different replicates varied up to about 10–20%.

Higher harmonics than the first provided interesting contrast between the bilayer and mica as the temperature was increased, and we will discuss a select few for illustrative purposes. For the 2nd harmonic (Fig. 4), contrast between the lipid and the mica in images obtained at 28–34 °C was quite small, and distinct populations of cantilever response at this frequency were not apparent in the histograms. At these temperatures, the typical response of the 2nd harmonic was on the order of 0.28–0.29 nm. However, the 2nd harmonic showed contrast between the transitioning domain of the bilayer at 34 °C and the surrounding lipid. Interestingly,

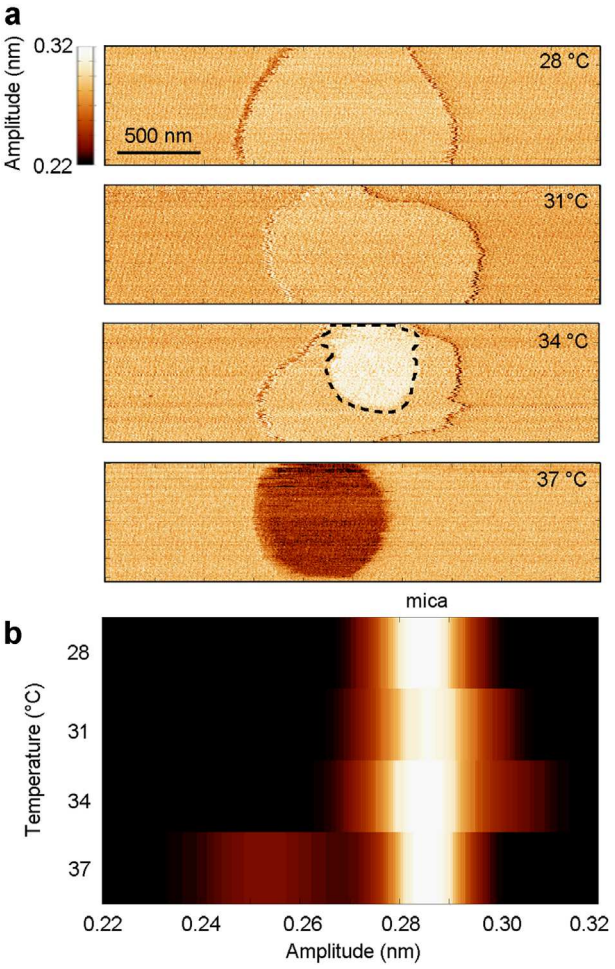

Fig 4. (**a**) Second harmonic AFM images of the same TBLE bilayer patch supported on mica taken at 28, 31, 34, and 37 °C. The dotted line in the image taken at 34 °C indicates a region of the bilayer undergoing a phase transition as determined from the topography image shown in Figure 1. The color bar is applicable to all images. (**b**) Histograms of all of the 2nd harmonic responses in the AFM images presented as a function of temperature. Brighter colors indicate a larger number of measurements corresponding to a specific response of the 2nd harmonic. Measurements corresponding to the mica substrate are indicated.

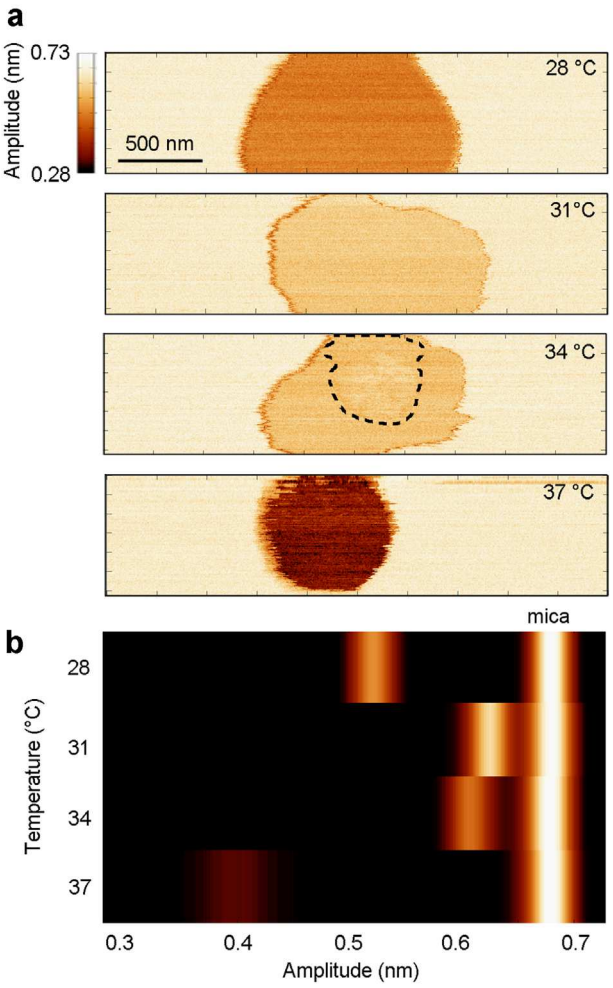

Fig 5. (**a**) Fifth harmonic AFM images of the same TBLE bilayer patch supported on mica taken at 28, 31, 34, and 37 °C. The dotted line in the image taken at 34 °C indicates a region of the bilayer undergoing a phase transition as determined from the topography image shown in Figure 1. The color bar is applicable to all images. (**b**) Histograms of all of the 5th harmonic responses in the AFM images presented as a function of temperature. Brighter colors indicate a larger number of measurements corresponding to a specific response of the 5th harmonic. Measurements corresponding to the mica substrate are indicated.

after the bilayer had gone through a phase transition (image taken at 37 °C), there was clear contrast in the 2nd harmonic image between the bilayer and mica with the bilayer associated with a smaller amplitude response (0.25 ± 0.03 nm) compared with the lower temperatures. Images based on the 5th harmonic (Fig. 5) provided distinct contrast between the bilayer and mica, with the bilayer always corresponding to a smaller amplitude response. At 28 °C the cantilever response associated with the 5th harmonic was 0.52 ± 0.05 nm, and this increased to 0.62 ± 0.08 nm and 0.61 ± 0.07 nm at 31 and 34 °C, respectively. However, the 5th harmonic was not particularly sensitive to the region of the bilayer undergoing transition at 34 °C, resulting in minimal contrast. The response of the 5th harmonic associated with the bilayer shifted to 0.37 ± 0.02 nm at 37 °C, which may be indicative of the phase transition in the bilayer. The response of the 5th harmonic was always consistent with the softer bilayer regions being associated with a smaller amplitude response compared with mica, and the magnitude of the cantilever response was approximately double compared to the 2nd harmonic. Imaging on the 6th harmonic (Fig. 6) resulted in negligible contrast from 28–34 °C, as only the edges of the bilayer were distinguishable from the mica. However, there was stark contrast between the bilayer and mica at 37 °C associated with the 6th harmonic. The magnitude of the 6th harmonic was also reduced to <0.26 nm. Images based on the response of the 7th harmonic (Fig. 7) provided distinct contrast between the

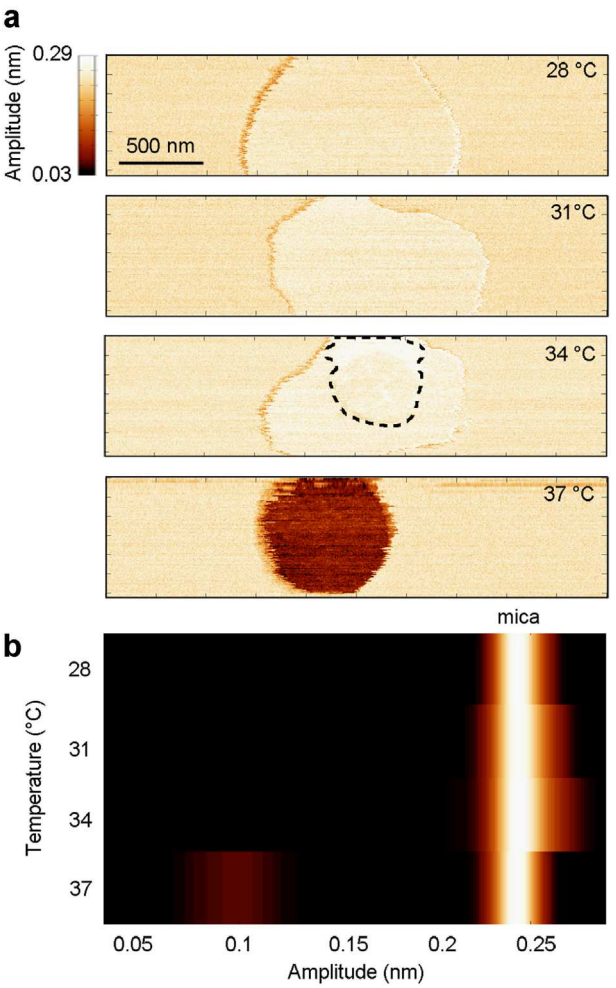

Fig 6. (**a**) Sixth harmonic AFM images of the same TBLE bilayer patch supported on mica taken at 28, 31, 34, and 37 ˚C. The dotted line in the image taken at 34 ˚C indicates a region of the bilayer undergoing a phase transition as determined from the topography image shown in Figure 1. The color bar is applicable to all images. (**b**) Histograms of all of the 6th harmonic responses in the AFM images presented as a function of temperature. Brighter colors indicate a larger number of measurements corresponding to a specific response of the 6th harmonic. Measurements corresponding to the mica substrate are indicated.

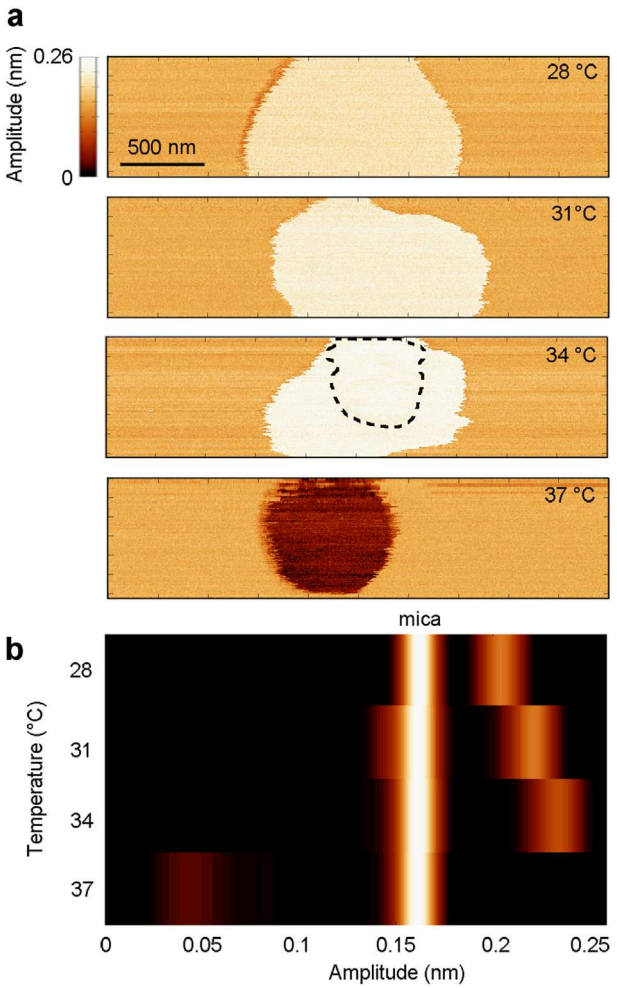

Fig 7. (**a**) Seventh harmonic AFM images of the same TBLE bilayer patch supported on mica taken at 28, 31, 34, and 37 ˚C. The dotted line in the image taken at 34 ˚C indicates a region of the bilayer undergoing a phase transition as determined from the topography image shown in Figure 1. The color bar is applicable to all images. (**b**) Histograms of all of the 7th harmonic responses in the AFM images presented as a function of temperature. Brighter colors indicate a larger number of measurements corresponding to a specific response of the 7th harmonic. Measurements corresponding to the mica substrate are indicated.

bilayer and mica at all temperatures. Unlike other harmonic images previously discussed, the amplitude response of the 7th harmonic was larger for the bilayer compared to mica at 28–34 ˚C. However, the amplitude response of the 7th harmonic associated with the bilayer shifted below that of mica at 37 ˚C, resulting in an inversion of contrast in the 7th harmonic images as the temperature was raised. Images can be produced for higher harmonics (for example the 10th and 15th harmonics shown in Fig. 8) with varying patterns of contrast as a function of temperature, but the magnitude of the response became quite small (<0.15 and 0.03 nm, respectively). Furthermore, the pattern of cantilever response as a function of temperature was very similar for harmonics ranging from the 12 to the 22nd harmonic (data not shown).

Collectively, obtained images demonstrate that higher harmonics can provide compositional contrast to varying degrees. However, unambiguous interpretation of the contrast afforded by higher harmonics is difficult. While the 2nd harmonic has been used to obtain compositional contrast of soft biological samples imaged in solution (Preiner *et al.*, 2007), it has been found that harmonics near the second eigenmode of the cantilever give larger responses and better contrast (Xu *et al.*, 2009). During the tapping event, the second eigenmode is momentarily excited, and this temporarily excites higher harmonics near this natural frequency,

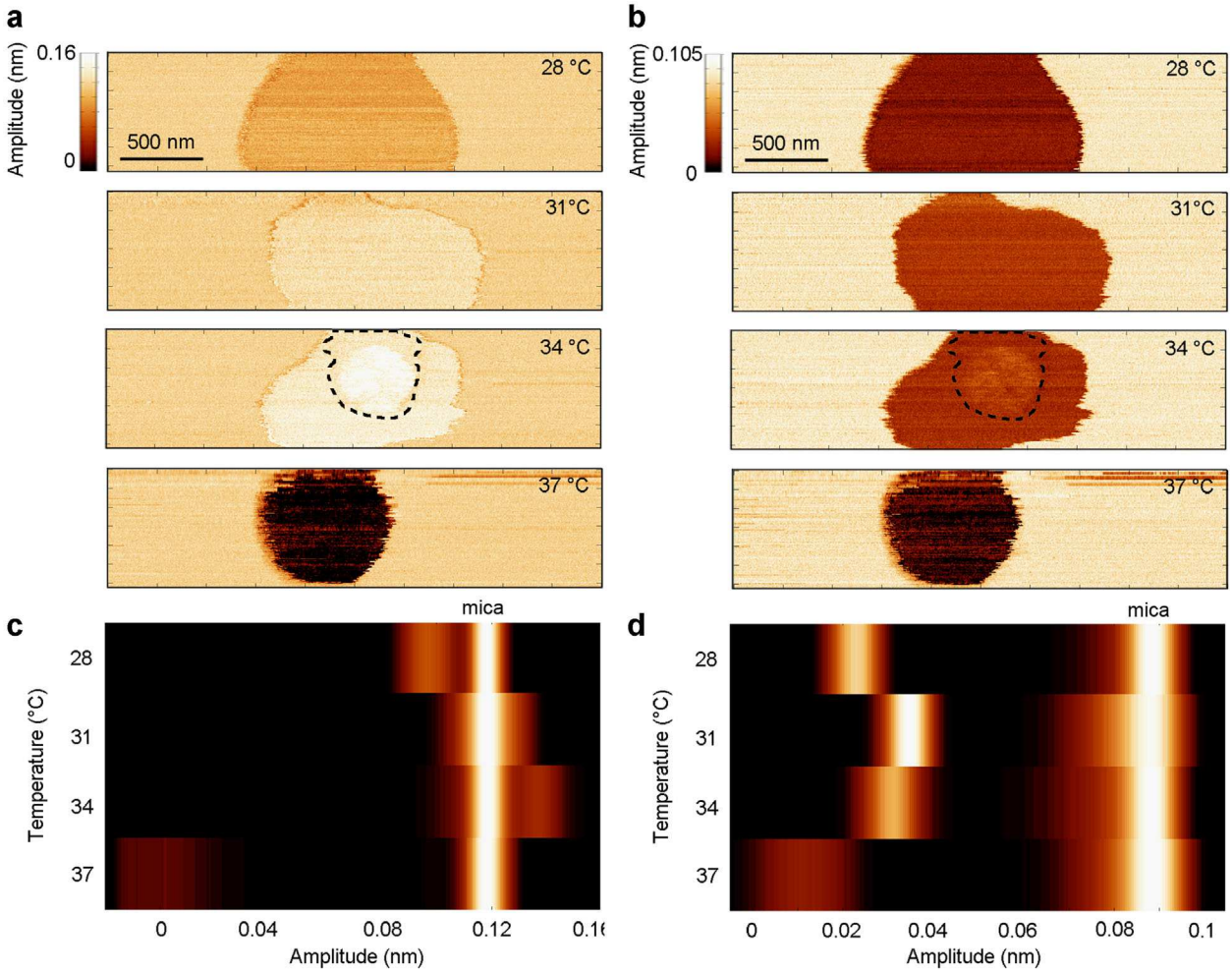

Fig 8. (**a**) Tenth and (**b**) fifteenth harmonic AFM images of the same TBLE bilayer patch supported on mica taken at 28, 31, 34, and 37 °C. The dotted line in the images taken at 34 °C indicate a region of the bilayer undergoing a phase transition as determined from the topography image shown in Figure 1. The color bar is applicable to all images. Histograms of all of the (**c**) 10th and (**d**) 15th harmonic responses in the AFM images presented as a function of temperature. Brighter colors indicate a larger number of measurements corresponding to a specific response of the 15th harmonic. Measurements corresponding to the mica substrate are indicated.

and these harmonics have been shown to be highly sensitive to local mechanical properties of the surface (Xu *et al.*, 2009). For the cantilever used in this study, the natural frequency of the second eigenmode was nearest to the 5th harmonic, resulting in the larger response associated with this harmonic. The higher sensitivity induced by proximity to the second eigenmode explains why the 5th harmonic response closely tracks the known temperature induced changes in the lipid bilayer patch. Similar to origins of phase contrast with soft, highly damped cantilevers (Melcher *et al.*, 2009), the contrast of this 5th harmonic is most likely derived from local elastic stiffness of the sample. In general, however, a single harmonic only provides partial information concerning the tip/sample interaction, but methods, such as force reconstruction, that combine the information stored in each individual harmonic may afford a more complete picture of the mechanical properties of samples.

Maximum Tapping Forces Reflect Temperature Induced Mechanical Changes in the Bilayer

It has been demonstrated by multiple numerical models and experiments that the maximum force (F_{max}), defined as the peak or largest positive force experienced between the tip and surface during the tapping event, increases with increasing elastic modulus of the sample (Shamitko-Klingensmith *et al.*, 2012; Burke *et al.*, 2013c; Guzman *et al.*, 2013). While this dependence is nonlinear and resembles a power law (Guzman *et al.*, 2013), it can be used to obtain contrast within an image based on relative elastic modulus (Legleiter *et al.*, 2011; Burke *et al.*, 2013a,b; Yates *et al.*, 2013). While the magnitude of the tapping force is influenced by imaging parameters, the relative value of F_{max} on the elastic modulus of the surface appears to be maintained. For example, increasing the spring constant of the cantilever results in a larger magnitude of imaging force,

but the power law dependence of F_{max} with the elastic modulus is preserved (Payam *et al.*, 2012; Chaibva *et al.*, 2014). Furthermore, the relative magnitude of F_{max} is also preserved with changes in the set point ratio and cantilever free amplitude (Kumar *et al.*, 2010; Shamitko-Klingensmith *et al.*, 2012). To evaluate the ability of F_{max} images to detect temperature induced mechanical changes in lipid bilayers associated with a phase transition, SPAM was used to invert the cantilever deflection signal into time-resolved tip/sample forces. The F_{max} associated with every tapping event was used to construct images of the bilayer patch on mica at different temperatures (Fig. 9). As before, the mica surface can be used as an internal reference point to compare F_{max} values at different temperatures. With this in mind, the relative magnitude of F_{max} associated with imaging the bilayer patch with respect to mica was reproduced from replicate to replicate. That is, the magnitude of F_{max} associated with imaging the bilayer patch was always smaller compared to the internal reference of mica, and there was always a pronounced shift to smaller values of F_{max} associated with imaging the bilayer after the temperature induced phase transition.

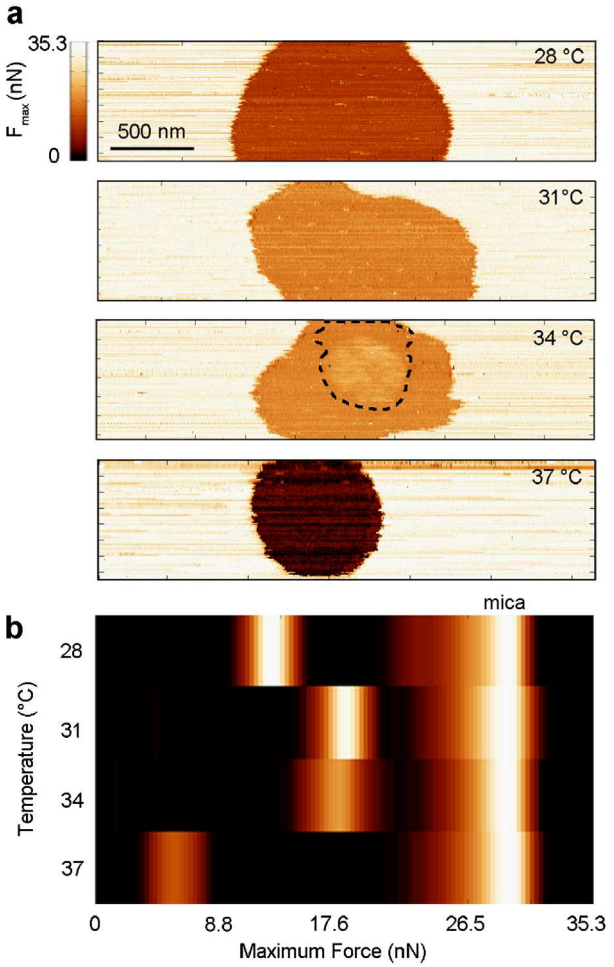

Fig 9. (**a**) F_{max} AFM images obtained from SPAM of the same TBLE bilayer patch supported on mica taken at 28, 31, 34, and 37 °C. The dotted line in the image taken at 34 °C indicates a region of the bilayer undergoing a phase transition as determined from the topography image shown in Figure 1. The color bar is applicable to all images. (**b**) Histograms of all of the F_{max} measurements in the AFM images presented as a function of temperature. Brighter colors indicate a larger number of measurements corresponding to a specific F_{max}. Measurements corresponding to the mica substrate are indicated.

At all temperatures, the F_{max} associated with the lipid bilayer was always smaller than the F_{max} associated with the bare mica substrate, as would be expected based on the relative rigidities of the surfaces (Shamitko-Klingensmith *et al.*, 2012). From 28–34 °C, a slight increase in F_{max} (12.4 ± 0.2 nN–16.9 ± 0.2 nN), indicating an initial increase in bilayer rigidity with increased temperature, was observed. This observation is consistent with the observed increase in bilayer height and the notion that increasing temperature raises lateral fluidity within bilayers, as previous studies suggested that higher fluidity corresponds with increased vertical rigidity in bilayers (Yip *et al.*, 2001; Shamitko-Klingensmith *et al.*, 2012). At 34 °C, faint contrast was observed for the region of the bilayer that began to transition to a more fluid phase, and this region appeared to be slightly more rigid (higher F_{max}). Once the bilayer underwent the apparent phase transition at 37 °C, F_{max} significantly declined (5.7 ± 0.1 nN). The decline of F_{max} at this higher temperature corresponds with the previously noted decrease in height, supporting the notion that the bilayer's phase transition resulted in a significantly lower elastic modulus. This reduced rigidity of the bilayer caused the cantilever tip to push deeper into the bilayer surface, compressing the bilayer and resulting in a smaller measured height, consistent with numerical simulations (Shamitko-Klingensmith *et al.*, 2012). Importantly, the relative values of F_{max} were always predictable and in accordance with the known rigidities of the bilayer and mica substrate.

Conclusions

While tapping mode AFM is widely used to obtain nanoscale images of soft samples in liquid, there has been considerable effort in developing methods that provide compositional contrast in AFM images. Here, we demonstrate the relative ability of phase, harmonic, and force reconstruction imaging to detect changes in the elastic modulus of a lipid bilayer patch supported on mica caused by a temperature induced phase transition. We made a direct comparison between these imaging techniques by simultaneously acquiring these different data types, ensuring that all images were acquired under the same experimental conditions. Using a priori knowledge concerning the sample and height images, we determined which imaging techniques were able to unambiguously reflect the temperature induced

mechanical change in the bilayer. The key mechanical change observed in the supported lipid bilayer was due to a phase transition induced between 34–37 °C, resulting in a highly compressible bilayer as confirmed by AFM height images.

While all of the techniques were able to provide compositional contrast associated with this phase transition, interpretation of this contrast was not always straightforward. Phase imaging suffered from contrast inversion between the known hard and soft regions of the surface in some replicates of the experiment. While a widely used technique for mapping mechanical differences on a surface, phase imaging suffers from the high dependence on the phase response to imaging parameters. Individual harmonic images exhibited a variety of response patterns at the different temperatures, with the largest cantilever response being associated with harmonic frequencies near an eigenmode of the cantilever, which for this particular experiment was the 5th harmonic. The response of the 5th harmonic, of all of the monitored harmonic frequencies, most accurately reflected the known temperature-induced change in bilayer mechanics, suggesting that harmonics near an eigenmode are particularly sensitive to changes in local surface properties. Force reconstruction was accomplished using SPAM, and changes in the F_{max} (or peak force) associated with imaging the bilayer correctly reflected the changes in elastic modulus of the lipid bilayer and was able to contrast subtle mechanical changes within the bilayer. This study was aided by the incorporation of an internal standard (exposed mica) so that relative changes in the response of these different imaging modes could be evaluated. Importantly, as the required data can be obtained simultaneously, combining these different imaging techniques can aid in ascertaining a more complete understanding of a sample's mechanical features.

References

Anczykowski B, Gotsmann B, Fuchs H, Cleveland JP, Elings VB. 1999. How to measure energy dissipation in dynamic mode atomic force microscopy. Appl Surf Sci 140: 376–382.

Bar G, Thomann Y, Brandsch R, Cantow HJ, Whangbo MH. 1997. Factors affecting the height and phase images in tapping mode atomic force microscopy. Study of phase-separated polymer blends of poly(ethene-co-styrene) and poly(2,6-dimethyl-1,4-phenylene oxide). Langmuir 13:3807–3812.

Basak S, Raman A. 2007. Dynamics of tapping mode atomic force microscopy in liquids: Theory and experiments. Appl Phys Lett 91:064107.

Burke KA, Hensal KM, Umbaugh CS, Chaibva M, Legleiter J. 2013a. Huntingtin disrupts lipid bilayers in a polyQ-length dependent manner. BBA-Biomembranes 1828:1953–1961.

Burke KA, Kauffman KJ, Umbaugh CS, Frey SL, Legleiter J. 2013b. The interaction of polyglutamine peptides with lipid membranes is regulated by flanking sequences associated with huntingtin. J Biol Chem 288:14993–15005.

Burke KA, Yates EA, Legleiter J. 2013c. Amyloid-forming proteins alter the local mechanical properties of lipid membranes. Biochemistry 52:808–817.

Chaibva M, Burke KA, Legleiter J. 2014. Curvature enhances binding and aggregation of huntingtin at lipid membranes. Biochemistry 53:2355–2365.

Cleveland JP, Anczykowski B, Schmid AE, Elings VB. 1998. Energy dissipation in tapping-mode atomic force microscopy. Appl Phys Lett 72:2613–2615.

Dong M, Husale S, Sahin O. 2009. Determination of protein structural flexibility by microsecond force spectroscopy. Nat Nanotechnol 4:514–517.

Ebeling D, Solares SD. 2013. Amplitude modulation dynamic force microscopy imaging in liquids with atomic resolution: Comparison of phase contrasts in single and dual mode operation. Nanotechnology 24.

Epand RM, Bottega R. 1987. Modulation of the phase transition behavior of phosphatidylethanolamine by cholesterol and oxysterols. Biochemistry 26:1820–1825.

Espinosa G, Lopez-Montero I, Monroy F, Langevin D. 2011. Shear rheology of lipid monolayers and insights on membrane fluidity. P Natl Acad Sci USA 108:6008–6013.

Garcia R, Herruzo ET. 2012. The emergence of multifrequency force microscopy. Nat Nanotechnol 7:217–226.

Garcia R, Magerle R, Perez R. 2007. Nanoscale compositional mapping with gentle forces. Nat Mater 6:405–411.

Garcia R, Tamayo J, San Paulo A. 1999. Phase contrast and surface energy hysteresis in tapping mode scanning force microsopy. Surf Ingerface Anal 27:312–316.

Guzman HV, Perrino AP, Garcia R. 2013. Peak forces in high-resolution imaging of soft matter in liquid. Acs Nano 7:3198–3204.

Hansma PK, Cleveland JP, Radmacher M, *et al*. 1994. Tapping mode atomic-force microscopy in liquids. Appl Phys Lett 64:1738–1740.

Herruzo ET, Garcia R. 2007. Frequency response of an atomic force microscope in liquids and air: Magnetic versus acoustic excitation. Appl Phys Lett 91:143113.

Hillenbrand R, Stark M, Guckenberger R. 2000. Higher-harmonics generation in tapping-mode atomic-force microscopy: Insights into the tip-sample interaction. Appl Phys Lett 76:3478–3480.

Hutter JL, Bechhoefer J. 1993. Calibration of atomic-force microscope tips. Rev Sci Instrum 64:1868–1873.

Jass J, Tjarnhage T, Puu G. 2000. From liposomes to supported, planar bilayer structures on hydrophilic and hydrophobic surfaces: An atomic force microscopy study. Biophys J 79: 3153–3163.

Kowalewski T, Legleiter J. 2006. Imaging stability and average tip-sample force in tapping mode atomic force microscopy. J Appl Phys 99:064903.

Kranenburg M, Smit B. 2005. Phase behavior of model lipid bilayers. J Phys Chem B 109:6553–6563.

Kučerka N, Nieh M-P, Katsaras J. 2011. Fluid phase lipid areas and bilayer thicknesses of commonly used phosphatidylcholines as a function of temperature. BBA-Biomembranes 1808:2761–2771.

Kumar B, Pifer PM, Giovengo A, Legleiter J. 2010. The effect of set point ratio and surface Young's modulus on maximum tapping forces in fluid tapping mode atomic force microscopy. J Appl Phys 107:044508.

Legleiter J, Fryer JD, Holtzman DM, Kowalewski T. 2011. The modulating effect of mechanical changes in lipid bilayers caused by ApoE-containing lipoproteins on Aβ induced membrane disruption. ACS Chem Neurosci 2:588–599.

Legleiter J, Park M, Cusick B, Kowalewski T. 2006. Scanning probe acceleration microscopy (SPAM) in fluids: Mapping mechanical properties of surfaces at the nanoscale. P Natl Acad Sci USA 103:4813–4818.

Leonenko Z, Finot E, Cramb D. 2006. AFM study of interaction forces in supported planar DPPC bilayers in the presence of

general anesthetic halothane. BBA-Biomembranes 1758: 487–492.
Magonov SN, Elings V, Whangbo MH. 1997. Phase imaging and stiffness in tapping-mode atomic force microscopy. Surf Sci 375:L385–L391.
Mansilla MC, Cybulski LE, Albanesi D, de Mendoza D. 2004. Control of membrane lipid fluidity by molecular thermosensors. J Bacteriol 186:6681–6688.
Melcher J, Carrasco C, Xu X, *et al*. 2009. Origins of phase contrast in the atomic force microscope in liquids. P Natl Acad Sci USA 106:13655–13660.
Melcher J, Xu X, Raman A. 2008. Multiple impact regimes in liquid environment dynamic atomic force microscopy. Appl Phys Lett 93:093111.
Milhiet P-E, Gubellini F, Berquand A, *et al*. 2006. High-resolution AFM of membrane proteins directly incorporated at high density in planar lipid bilayer. Biophys J 91:3268–3275.
Mueller DJ, Engel A. 2007. Atomic force microscopy and spectroscopy of native membrane proteins. Nat Protoc 2:2191–2197.
Pan J, Tristram-Nagle S, Ku N, Nagle JF. 2008. Temperature dependence of structure, bending rigidity, and bilayer interactions of dioleoylphosphatidylcholine bilayers. Biophys J 94:117–124.
Payam AF, Ramos JR, Garcia R. 2012. Molecular and nanoscale compositional contrast of soft matter in liquid: Interplay between elastic and dissipative interactions. ACS Nano 6: 4663–4670.
Pifer PM, Yates EA, Legleiter J. 2011. Point mutations in Aβ result in the formation of distinct polymorphic aggregates in the presence of lipid bilayers. PLoS ONE 6:e16248.
Preiner J, Tang J, Pastushenko V, Hinterdorfer P. 2007. Higher harmonic atomic force microscopy: Imaging of biological membranes in liquid. Phys Rev Lett 99:046102.
Putman CAJ, Vanderwerf KO, Degrooth BG, Vanhulst NF, Greve J. 1994. Tapping mode atomic-force microscopy in liquid. Appl Phys Lett 64:2454–2456.
Revenko I, Proksch R. 2000. Magnetic and acoustic tapping mode microscopy of liquid phase phospholipid bilayers and DNA molecules. J Appl Phys 87:526–533.
Sahin O, Yaralioglu G, Grow R, *et al*. 2004. High-resolution imaging of elastic properties using harmonic cantilevers. Sensors and Actuators a-Physical 114:183–190.
Sarioglu AF, Magonov S, Solgaard O. 2012. Tapping-mode force spectroscopy using cantilevers with interferometric high-bandwidth force sensors. Appl Phys Lett 100:053109.
Sarioglu AF, Solgaard O. 2011. Modeling, design, and analysis of interferometric cantilevers for time-resolved force measurements in tapping-mode atomic force microscopy. J Appl Phys 109:064316.
Scott WW, Bhushan B. 2003. Use of phase imaging in atomic force microscopy for measurement of viscoelastic contrast in polymer nanocomposites and molecularly thick lubricant films. Ultramicroscopy 97:151–169.
Shamitko-Klingensmith N, Molchanoff KM, Burke KA, Magnone GJ, Legleiter J. 2012. Mapping the mechanical properties of cholesterol-containing supported lipid bilayers with nanoscale spatial resolution. Langmuir 28:13411–13422.
Simons K, Vaz WLC. 2004. Model systems, lipid rafts, and cell membranes. Annu Rev Bioph Biom 33:269–295.
Stark M, Möller C, Müller DJ, Guckenberger R. 2001. From images to interactions: High-resolution phase imaging in tapping-mode atomic force microscopy. Biophys J 80:3009–3018.
Stark M, Stark RW, Heckl WM, Guckenberger R. 2002. Inverting dynamic force microscopy: From signals to time-resolved interaction forces. P Natl Acad Sci USA 99:8473–8478.
Stark RW, Hecki WM. 2003. Higher harmonics imaging in tapping-mode atomic-force microscopy. Rev Sci Instrum 74:5111.
Suresh S, Edwardson JM. 2010. Phase separation in lipid bilayers triggered by low pH. Biochem Bioph Res Co 399: 571–574.
Van Dijck PWM, De Kruijff B, Van Deenen LLM, De Gier J, Demel RA. 1976. The preference of cholesterol for phosphatidylcholine in mixed phosphatidylcholine-phosphatidylethanolamine bilayers. BBA-Biomembranes 455:576–587.
van Noort SJT, Willemsen OH, van der Werf KO, de Grooth BG, Greve J. 1999. Mapping electrostatic forces using higher harmonics tapping mode atomic force microscopy in liquid. Langmuir 15:7101–7107.
vanMeer G, Voelker DR, Feigenson GW. 2008. Membrane lipids: Where they are and how they behave Nat Rev Mol Cell Bio 9: 112–124.
Voitchovsky K, Contera SA, Kamihira M, Watts A, Ryan JF. 2006. Differential stiffness and lipid mobility in the leaflets of purple membranes. Biophys J 90:2075–2085.
Xu X, Melcher J, Basak S, Reifenberger R, Raman A. 2009. Compositional contrast of biological materials in liquids using the momentary excitation of higher eigenmodes in dynamic atomic force microscopy. Phys Rev Lett 102: 060801.
Yates EA, Owens SL, Lynch MF, *et al*. 2013. Specific domains of abeta facilitate aggregation on and association with lipid bilayers. J Mol Biol 425:1915–1933.
Yip CM, Elton EA, Darabie AA, Morrison MR, McLaurin J. 2001. Cholesterol, a modulator of membrane-associated Aβ-fibrillogenesis and neurotoxicity. J Mol Biol 311:723–734.
Zitzler L, Herminghaus S, Mugele F. 2002. Capillary forces in tapping mode atomic force microscopy. Phys Rev B 66: 155436.